



Decreased peak alpha frequency and impaired visual evoked potentials in first episode psychosis

Murphy Michael^{a,b,*}, Öngür Dost^{a,b}

^a Harvard Medical School, Boston, MA, United States of America

^b McLean Hospital, Belmont, MA, United States of America

ARTICLE INFO

Keywords:

EEG
First episode psychosis
Resting state
Schizophrenia
Alpha
Steady-state evoked potentials

ABSTRACT

Abnormal spontaneous and evoked oscillations have been reported in several studies of patients with psychotic disorders. Resting alpha power and peak alpha frequency may be decreased in patients with psychosis. We used high-density EEG (hd-EEG) to record resting-state data and steady-state visual evoked potentials (SSVEPs) in patients with first episode psychosis (FEP) and healthy controls to compare brain resonances across multiple frequencies. We recorded hd-EEG (128 channels) from 22 FEP patients and 22 healthy controls during eyes-closed resting state and eyes-closed photic stimulation at 1 Hz, 4 Hz, 10 Hz, 20 Hz, and 40 Hz. Alpha power, peak alpha frequency, and SSVEP amplitude were analyzed using ANOVA and statistical non-parametric mapping. We found that FEP patients had lower peak alpha frequencies (9.72 Hz vs 10.40 Hz, $p = .02$, Cohen's $d = 0.73$) and this decrease was driven by slowing over the central and posterior scalp. There was no difference in alpha power. Alpha waves propagated primarily from anterior to posterior and that propagation was slowed in patients. During SSVEP, patients had smaller increases in EEG power in the stimulation band ($F_{(1,184)} = 5.3$, $p = .02$). Patients had attenuated responses to SSVEP stimulation at alpha, beta and gamma frequencies. The gamma response was partially preserved in patients who also had depressive symptoms. We conclude that even in early stages of illness, psychotic disorders are associated with decreased alpha peak frequency and impaired evoked resonances. These findings implicate multiple patterns of dysconnectivity in cortico-cortico and cortico-thalamic networks in FEP.

1. Introduction

During periods of quiet rest, the human electroencephalogram (EEG) is dominated by large bursts of alpha (8–12 Hz) band activity. This is a well-described phenomenon that was first noted by Hans Berger during his initial investigations with EEG (Millett, 2001). Since these reports, a large body of literature has been produced detailing the nature of the alpha rhythm, its relationship with the resting state, and its perturbation in neurological and psychiatric illnesses (Hughes and Crunelli, 2005).

The basic neurophysiology of the alpha rhythm is incompletely understood. Neuroimaging and invasive studies indicate that the alpha rhythm is generated by a complex interplay between thalamic and cortical pacemakers and propagates via short and long range cortico-cortical, cortico-thalamic, and thalamo-cortical connections (Hughes and Crunelli, 2005; Schreckenberger et al., 2004). Thalamic driving of alpha activity is thought to arise from high-threshold burst firing within thalamocortical neurons in the lateral geniculate nucleus (LGN) and

pulvinar nucleus which then project to the posterior cortex (Hughes and Crunelli, 2005). However, the thalamus is not the sole pacemaker of the alpha rhythm. High-threshold bursting within these thalamic nuclei is tuned by corticothalamic input (Hughes and Crunelli, 2005). Furthermore, EEG and electrocorticography studies have shown that alpha waves propagate from anterior-to-posterior and from the cortex to the thalamus (Ito et al., 2005; Bahramisharif et al., 2013; Halgren et al., 2017; Manjarrez et al., 2007). It may be that alpha activity in the prefrontal cortex, modulated by attentional and cognitive demands, propagates via short-range connections to adjacent cortical areas and via long-range connections to the thalamus. The thalamic alpha pacemaker is entrained by this input. The thalamic pacemaker entrains downstream alpha waves in the posterior cortex. Thus frontal regions drive posterior alpha activity via both cortico-cortical and cortico-thalamo-cortical connections. This is consistent with a proposed role of the alpha rhythm in mediating top-down cognitive control (Becker et al., 2017; Hanslmayr et al., 2011; Samaha et al., 2015).

Given the complexity of the neural systems underlying the alpha

* Corresponding author at: McLean Hospital, Mailstop 108, 115 Mill Street, Belmont, MA 02478, United States of America
E-mail address: mmurphy@mgh.harvard.edu (M. Murphy).

<https://doi.org/10.1016/j.nicl.2019.101693>

Received 8 August 2018; Received in revised form 29 November 2018; Accepted 27 January 2019

Available online 21 February 2019

2213-1582/ © 2019 The Authors. Published by Elsevier Inc. This is an open access article under the CC BY-NC-ND license (<http://creativecommons.org/licenses/by-nc-nd/4.0/>).

rhythm, it is perhaps not surprising that these systems are disrupted in patients with psychotic disorders. Multiple studies have reported that patients with schizophrenia have decreased resting state alpha power, but there are also reports of increased alpha power (Clementz et al., 1994; Karson et al., 1988; Goldstein et al., 2015; Harris et al., 2006; Boutros et al., 2008; Narayanan et al., 2014). Decreased alpha power has been reported in a variety of psychiatric and neurological illnesses as well as in healthy relatives of individuals with psychotic disorders (Clementz et al., 1994; Boutros et al., 2008; Narayanan et al., 2014; Basar et al., 2012; Karadağ et al., 2003; Prinz and Vitiello, 1989; Linas et al., 1999). Alpha power is decreased in medication-naïve first episode schizophrenia patients as well as in chronic, medicated patients and euthymic bipolar patients without psychotic symptoms (Clementz et al., 1994; Goldstein et al., 2015; Basar et al., 2012). It is unlikely to be a medication effect given that patients with affective disorders who use antipsychotic medication appear to be indistinguishable from controls (Goldstein et al., 2015). In addition to changes in absolute alpha power, the nature of the alpha activity is also altered in schizophrenia. Specifically, studies of resting EEG of patients have also shown decreased peak alpha frequency (Harris et al., 2006). Peak alpha frequency may be inversely correlated with duration of illness, but decreases are detected in first-episode patients (Clementz et al., 1994; Goldstein et al., 2015).

The resting-state data suggests disruption in the alpha-generating networks in psychotic disorders but are ambiguous as to the specific causal dysfunction. One possibility is that patients with psychotic disorders have an intrinsically slowed alpha rhythm as a result of persistent hyperpolarization of thalamocortical neurons caused by inappropriate corticothalamic feedback and/or dysfunction within the thalamocortical neurons themselves (Hughes and Crunelli, 2005). In this case, the “alpha” activity might extend into the slower theta band (Linas et al., 1999). Alternatively, there could be slowing of intrinsic alpha pacemakers or relatively impaired propagation of faster alpha activity. Steady-state visual evoked potentials (SSVEPs), a measure of the entrainment of brain rhythms produced by repeatedly presenting a visual stimulus at a fixed frequency, can further clarify the disruption in this system (Rice et al., 1989). The SSVEP response is mediated by the magnocellular and parvocellular neurons within the LGN as well as pulvinar nuclei projections onto visual cortex (Vialatte et al., 2010). SSVEPs can be elicited using a stimuli which preferentially target different components of this pathway (Wada et al., 1995). SSVEPs do not rely on any potential frontal cortex pacemaker, although the amplitude of the SSVEP response may be modulated by attention (Hanslmayr et al., 2011; Müller and Hübner, 2002). There is a large body of literature describing abnormal SSVEP responses in schizophrenia. In particular, the photic driving response which refers to the ability of high-intensity periodic flashing light to induce harmonic oscillations in the EEG via a magnocellular-mediated process, is known to be disrupted in patients with schizophrenia (Jin et al., 1990, 1997; Butler and Javitt, 2005).

There is a growing consensus that psychotic disorders are overlapping entities that exist on a continuum (Craddock and Owen, 2007). A first episode of psychosis results from combinations of genetic, developmental and environmental events as well as complex homeostatic responses to these events (Craddock and Owen, 2007; Corvin and Harold, 2015; Ripke et al., 2014; Lisman et al., 2008). Such heterogeneity would likely vary over time and may be why diagnostic categories are highly unstable early in the course of psychotic illness (Shinn et al., 2017). Furthermore, even in individuals with a stable, well-established diagnosis, there is considerable variability in clinical outcome that cannot be entirely explained by treatment adherence or co-morbid substance use (Tohen et al., 2003). Therefore, in this study, we considered patients with first episode psychosis (FEP) as a distinct category, irrespective of whether they were diagnosed with affective or non-affective psychosis. In this way, we hoped to identify features that were common to patients with a recent onset of psychotic symptoms

and that are unlikely to be related to prolonged medication exposure or the impact of disease chronicity longer than 3 years. Within these patients, we used a recently developed five-factor analysis of the Positive and Negative Symptom Scale (PANSS) in order to more precisely characterize symptom burden at the time of EEG recording (Wallwork et al., 2012).

We used resting-state high-density EEG (hd-EEG) and SSVEPs to probe physiology in FEP patients. Hd-EEG allowed us to more precisely delineate regional changes in alpha power and assess abnormalities in traveling wave characteristics obscured by more limited EEG montages. Based on prior findings and theoretical considerations, we hypothesized that FEP patients would have decreased alpha power and alpha frequency as well as decreased SSVEP responses to alpha, beta, and gamma stimulation consistent with abnormal thalamic functioning. We also hypothesized that the topography of these deficits would be consistent with disrupted cortico-cortical propagation of the alpha wave.

2. Methods and materials

2.1. Participants

Twenty five patients with first-episode psychosis (within 3 years of initial diagnosis) were recruited from inpatient units and outpatient clinics at McLean Hospital. Age-matched controls with no history of current or previous mental illness were recruited from advertisements posted in the community (Table 1). We excluded individuals with a history of head injury, neurological disorders, prior electroconvulsive therapy, and active major medical illness. All study procedures were approved by the Institutional Review Board of the Partners HealthCare System. Participants provided written informed consent. Patients

Table 1

Demographic information about patients and controls. Values shown are mean \pm standard error of the mean. Sz = schizophrenia, Sza = schizoaffective, BP = bipolar with psychotic features.

	HC	FEP
n	22	22
Age (years)	23.1 \pm 2.7	22.0 \pm 2.7
Sex (male/female)	11/11	15/7
PANSS Positive Factor		7.5 \pm 2.8
PANSS Negative Factor		11.4 \pm 3.6
PANSS Disorganized Factor		4.7 \pm 2.1
PANSS Excited Factor		5.8 \pm 2.3
PANSS Depressed Factor		4.4 \pm 1.6
Chlorpromazine (CPZ) equivalents (mg)		232.7 \pm 181.0
	Chlorpromazine (CPZ) equivalents (mg)	% Taking Mood Stabilizer
SZ/SZA	7 360.4 \pm 73.4	50
BP		
Manic	7 209.6 \pm 51.7	85.7
Depressive	1 0	100
Mixed	2 275.0 \pm 125.0	100
Euthymic	2 133.5 \pm 133.5	50
MDD w/psychosis	1 133	0
Psychosis NOS	2 200.0 \pm 200.0	0
No current or past substance use disorders	8	
Alcohol use disorder		
Active	3	
In remission	0	
Cannabis use disorder		
Active	9	
In remission	2	
Opioid use disorder		
Active	1	
In remission	1	

recruited from inpatient units had an independent evaluation of their capacity to consent to research performed by independent clinicians. Data from 3 patients and 3 controls were excluded from the study because of excessive EEG artifact (persistent broadband signal in all channels). Five additional patients did not complete the visual steady state evoked potentials portion and one patient completed all but the 40 Hz stimulation.

2.2. Procedure

Patient participants completed a video-taped Structured Clinical Interview for the Positive and Negative Symptom Scale (SCI-PANSS). Patient participants also completed the Structured Clinical Interview for DSM-5. After interviews and collection of demographic data, the EEG cap was applied (see below). For resting state data, participants were instructed to fixate on a point approximately 90 cm in front of them and to remain still and relaxed with eyes closed for three minutes. This was then repeated with eyes open. Following the resting state recordings, steady-state visual evoked potential (SSVEP) data was collected for 2 min blocks at 1, 4, 10, 20, and 40 Hz. For each block, we instructed participants to fixate on a lamp 90 cm in front of them and close their eyes. The lamp was connected to a photic stimulator (PS-22, Grass Technologies, Warwick, RI) which delivered a sinusoidal light flicker (peak luminance 1200 cd/m²) at the appropriate frequency. Each SSVEP block was separated by at least one minute in order to minimize carry-over effects.

2.3. Clinical characterization

The recorded PANSS interviews were scored offline (Kay et al., 1987). The PANSS is widely used in psychosis research, although the factor structure of the scale is controversial. While the original authors of the PANSS suggested three subscales/factors, multiple subsequent studies have suggested that five or even seven factors are needed (Wallwork et al., 2012; van der Gaag et al., 2006). Multiple weighting algorithms to generate factors have been proposed. In this paper, we use a five-factor model derived from a consensus of 29 previously published five-factor models (Wallwork et al., 2012). These factors are Positive, Negative, Disorganized, Excited, and Depressed. The model incorporates 20 of the 40 PANSS items. One notable omission is the Paranoia item (P6). We therefore analyzed this item independently. Because a previous report suggested that the SSVEP response may be correlated with hallucinations, we also examined the PANSS Hallucination item independently (Krishnan et al., 2005).

2.4. Electroencephalography

EEG data were collected using a Geodesic Sensor Net (Electrical Geodesics Incorporated, Eugene, OR) with 128 Ag-AgCl electrodes. Data were collected at 1 kHz sampling rate with a vertex reference using the NetStation software package (EGI) in an electrically shielded room while patients sat in a comfortable chair. Impedances were maintained below 65 k Ω . EEG data were preprocessed by 0.5–50 Hz band-pass filtering and spline interpolation of bad channels identified by visual inspection and then exported to MATLAB (MathWorks, Natick MA). A semi-automated procedure was then used to identify artefactual segments of data and any additional bad channels. Following artifact rejection and bad channel interpolation, the data was then re-referenced to the global average as has been done in previous studies of resting EEG activity in schizophrenia (Goldstein et al., 2015; Hirano et al., 2015). For frequency analyses, we estimated the power spectral density using Welch's method with non-overlapping Hamming windows of 2 s in length which were then averaged to generate the power spectral density.

2.5. Traveling wave analysis

EEG data were referenced to linked mastoids and band-pass filtered from 8 to 12 Hz. A virtual average channel was created by averaging across all channels. Zero-crossings were detected in this average channel (Fig. 3a). The timing of the zero-crossings was used to segment the data. Intervals between positive-going zero-crossings and their subsequent negative-going zero-crossing were used to identify positive half-waves and intervals between negative going zero-crossings and subsequent positive going zero-crossings were used to identify negative half-waves. Within each half-wave interval, we calculated the timing of the local maxima/minima for each channel that had a maximum/minimum not on the edge of the interval. If any channel had multiple local extrema within the window, we identified that wave as a multi-peak wave and excluded it from further analysis. There was no difference between the percentage of multi-peak waves in controls (6.78% \pm 0.73%) vs patients (7.81% \pm 0.59%, $p = .28$ unpaired t -test). This left us with 42,433 half waves in the controls and 33,345 half waves in patients. For each half-wave, the first 10% of peaks were considered the origin. This approach of identifying multiple channels as the origin reduces the precision but makes the algorithm more robust to spurious peaks (Murphy et al., 2009). For each channel that had a peak during the half-wave, we calculated the latency between the timing of the first peak and the peak in that channel as in (Massimini, 2004).

2.6. Source modeling

Source modeling was performed using the Brainstorm toolbox for MATLAB (Tadel et al., 2011). Standardized electrode locations were co-registered to a magnetic resonance image of an individual whose head approximates the Montreal Neurological Institute head. The co-registered electrode locations and anatomical MRI were used to create a boundary-element head model. Cortical current sources were modeled using the standardized low resolution electromagnetic topography (sLORETA) algorithm (Pascual-Marqui, 2002).

2.7. Statistical analyses

For topographic analyses and power spectral density comparisons, family-wise error rate was controlled at a level of 0.05 by using statistical nonparametric mapping (SnPM) and SnPM suprathreshold cluster analyses (Nichols and Holmes, 2001). For each comparison, we ran 10,000 randomly selected permutations. We calculated covariance and correlation matrices with the five PANSS factors, EEG peak alpha frequency, alpha wave propagation speed and SSVEP responses at each of the stimulation frequencies and their harmonics.

3. Results

3.1. Peak alpha frequency, but not power, is decreased in patients with first episode psychosis

For each subject in the eyes-closed resting state, we estimated the power spectral density (PSD) in each channel and then calculated the average PSD across channels. Analysis of these mean PSDs showed no statistically significant differences between patients and controls (Fig. 1). Both groups had a peak in the alpha frequency range (Fig. 1A). We found no topographic differences between the two groups in either individual channel (tested with SnPM) or cluster analysis (tested with SnPM suprathreshold cluster testing) (Fig. 1B). To quantify variability in alpha power, we divided the data into 4 s windows, calculated the alpha power within each window, and then calculated the variance across windows for each subject. We found no statistically significant differences in variance between controls (2.03 \pm 0.51) and patients (0.99 \pm 0.27) ($p = .08$, unpaired t -test).

In order to calculate the individual alpha peaks, for each subject and

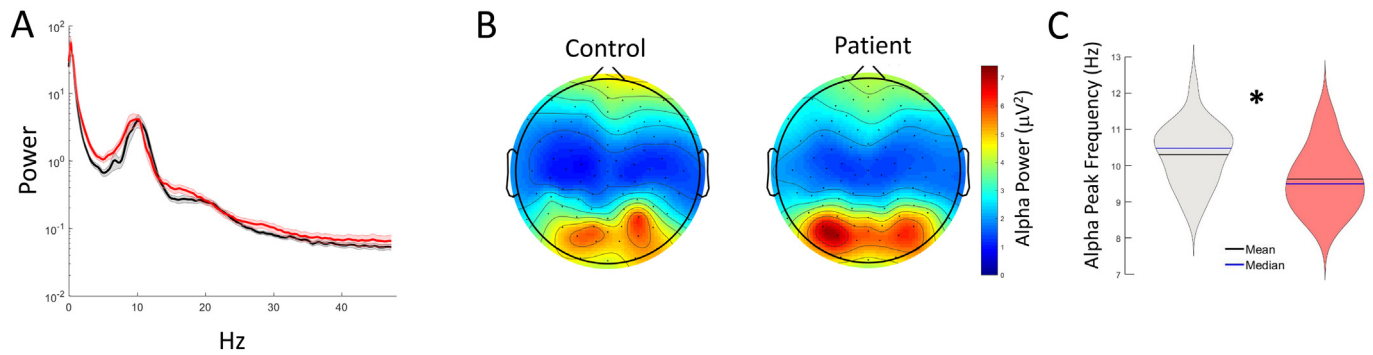


Fig. 1. Alpha power and peak frequency. A) Mean power spectra across all channels from 0 to 49 Hz were calculated for controls (black) and patients (red). Shaded areas are standard error of the mean at each frequency. There were no statistically significant differences between patients and controls in any frequency bin. B) Topoplots of control and patient alpha (8–12 Hz) power. There were no statistically significant differences in any channel. C) Violin plots of the mean alpha peak frequency across all channels in controls (gray) and patients (red). * $p = .011$, unpaired t-test. Patients had significantly lower peak alpha frequencies (9.72 ± 0.18 Hz vs 10.40 ± 0.18 Hz, Cohen's $d = 0.80$).

each channel in the eyes-closed resting state, we identified the frequency bin in the alpha range (8–12 Hz) with the greatest power. This was the individual alpha peak for that subject and channel. We then calculated the mean individual alpha peak by averaging across channels. Patients had a statistically significant lower peak alpha frequency (9.72 ± 0.18 Hz) than controls (10.40 ± 0.18 Hz) ($p = .011$, unpaired t-test, Cohen's $d = 0.80$, Fig. 1C). There were no statistically significant between-group differences in average power across channels at individual alpha peaks.

We note that within the patient group peak alpha frequency was not correlated with chlorpromazine equivalents ($r = -0.25$, $p > .26$), mood stabilizers (lithium, divalproic acid, topiramate, $r = 0.20$, $p > .37$), antidepressant medications (bupropion and selective serotonin reuptake inhibitors, $r = -0.26$, $p > .24$) or benzodiazepines ($r = 0.13$, $p > .56$). In our study, all patients who were taking antipsychotic medication were taking atypical antipsychotics. In previous work, one atypical antipsychotic, quetiapine, has been shown to decrease alpha power in healthy controls (Yoshimura et al., 2007). Two patients in this study were taking quetiapine. Excluding these subjects from the analysis did not change our findings of decreased peak alpha frequency (9.81 ± 0.21 Hz, $p = .041$, unpaired t-test when compared to controls) and unchanged alpha power. The two patients taking quetiapine did not statistically different alpha power (2.59 ± 1.62 vs 3.10 ± 0.51) or peak alpha frequency (10.13 ± 0.12 Hz vs 9.81 ± 0.21 Hz) than the remaining patients, but we note that this study was not designed or powered to detect such differences.

We repeated these analyses with the eyes-open resting state data. We again found no statistically significant power differences between patients and controls. We also found that in the eyes-open condition, patients again had statistically significant lower peak alpha frequency (9.03 ± 0.29 Hz) than controls (10.17 ± 0.24 Hz) ($p = .0037$, Cohen's $d = 0.98$). However, for the eyes-open experiment, data from four additional patients was rejected because of persistent movements, eye blinks, and other artifacts. Therefore, we restricted our remaining analyses to the eyes-closed data.

3.2. Decreased peak alpha frequency is driven by central, posterior, and temporal cortical regions

In order to identify cortical regions that showed slowed alpha rhythms, we used sLORETA to create cortical current models of the EEG data and calculated the mean PSD across all cortical voxels (Fig. 2). Mean source space PSDs and EEG PSDs were similar in appearance but patients did show an increase in power in several frequency bins in the theta band range, in particular from 6 to 7.5 Hz (SnPM, p -values .039–0.049). We did not find power differences in the alpha range. We then calculated the peak alpha frequency for each cortical voxel and

the mean peak alpha frequency for each subject. To assess effect of sLORETA on peak alpha frequency subject we compared the peak alpha frequency in the EEG space to the peak alpha frequency in source space for each subject (Fig. 2B). EEG and source individual alpha peak frequencies were highly correlated (Pearson's $r = 0.828$, $p < .00001$) although source space frequencies were generally higher. In source space, there was also a reduction in peak alpha frequency in patients vs controls (9.35 ± 0.23 Hz, 10.06 ± 0.23 Hz, $p = .033$, unpaired t-test, Cohen's $d = 0.66$).

In both controls and patients, peak alpha frequency was lowest in prefrontal cortex. We evaluated topographic differences in peak alpha frequency between the two groups using SnPM suprathreshold cluster testing and found a large cluster of cortical voxels that had slower peak alpha frequencies in patients compared to controls ($p = .002$). This cluster included portions of frontal, parietal, temporal, and occipital cortex (Fig. 2c). Notably, prefrontal cortex was spared as was most somatosensory cortex.

3.3. Propagation of alpha waves is impaired in patients with first episode psychosis

We tracked the origins and propagation of alpha waves using the timing of local maxima and minima relative to zero-crossings in the mean mastoid-referenced channel as described in the Methods section (Fig. 3). A representative wave is shown Fig. 3b. This wave began over the front of the scalp and traveled posteriorly. Overall, controls and patients had a similar pattern of alpha wave origins with most half-waves originating in a hotspot extending from the anterior-most scalp laterally to the ears and the fewest originating in a cold-spot over central regions of the scalp (Fig. 3).

For each alpha half-wave, we calculated the difference between the timing of the positive peak in each channel and the timing of the first identified peaks for that wave (Fig. 3). We calculated the average delay at each channel by averaging across waves. We found a cluster of posterior-central channels with higher delays in patients compared to controls indicating slower alpha wave propagation to these regions ($p = .045$, SnPM suprathreshold cluster test). In patients, the rate of propagation was not correlated with chlorpromazine equivalents ($r = -0.25$, $p > .26$), mood stabilizers (lithium, divalproic acid, topiramate, $r = -0.14$, $p > .53$), antidepressant medications (bupropion and selective serotonin reuptake inhibitors, $r = -0.26$, $p > .24$) or benzodiazepines ($r = -0.31$, $p > .16$).

3.4. Patients showed decreased responses to steady state visual stimulation

In steady-state visual evoked potential (SSVEP) experiments, we analyzed mean eyes-closed EEG power across channels in a 1 Hz bin

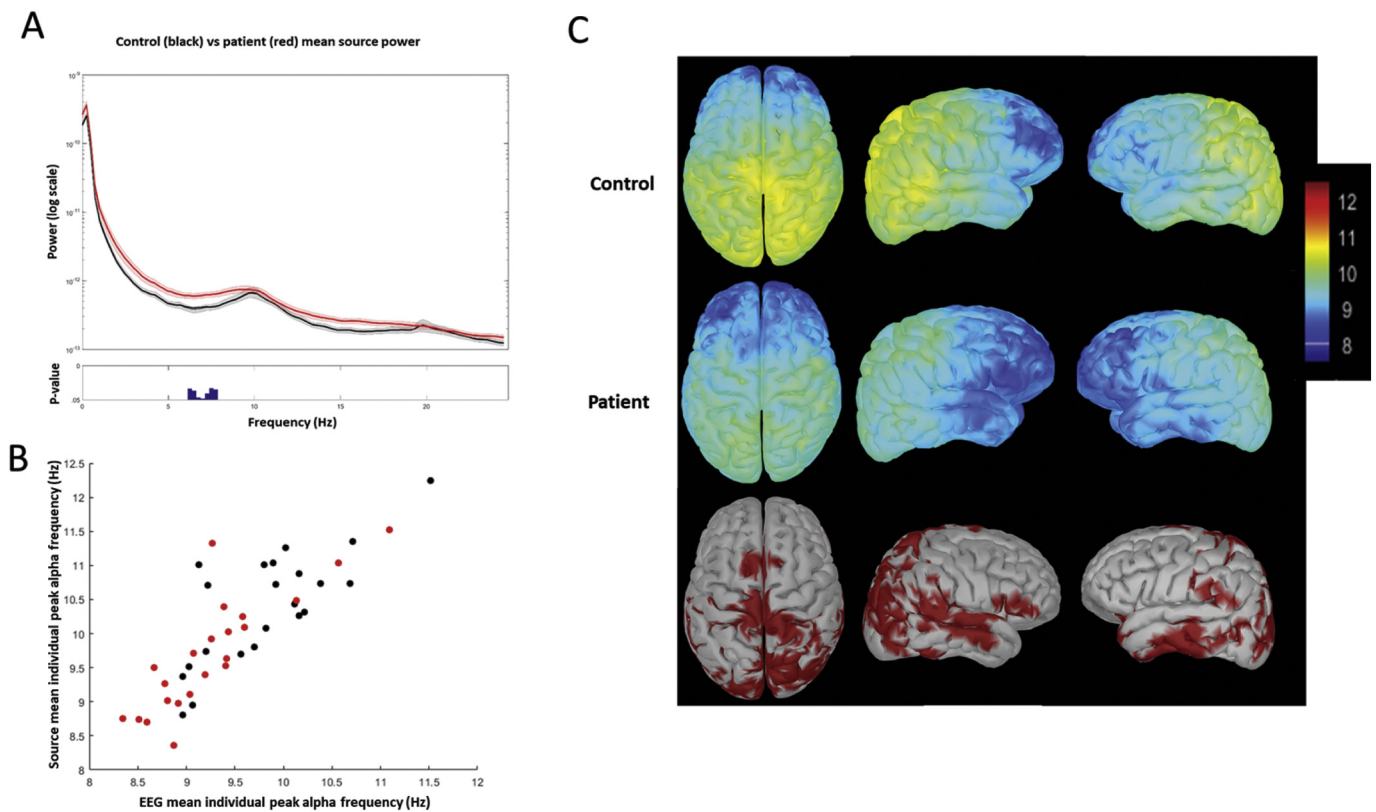


Fig. 2. Source space analysis. A) Mean power spectra across all voxels from 0 to 30 Hz for controls (black) and patients (red). Shaded areas are standard error of the mean at each point. Lower panel is p value in each bin calculated by statistical non-parametric mapping. There was increased theta power in patients compared to controls. B) Mean EEG peak alpha frequency plotted vs mean source peak alpha frequency. The peak alpha frequencies derived from EEG are highly correlated with peak alpha frequencies derived from source space transformed EEG data (Pearson's $r = 0.828$, $p < .00001$). C) Cortical map of alpha peak frequency. Average alpha peak frequency in control (top row) and patient (middle row) groups. The bottom row shows voxels that have a statistically lower peak alpha frequency in the patient population (SnPM suprathreshold cluster test, $p = .002$). These areas include medial frontal cortex, parietal cortex, temporal cortex, and occipital cortex.

centered on the stimulation frequency in the stimulation condition compared to the eyes closed baseline condition (Fig. 4). In both groups, 1 Hz stimulation was unable to produce a clear increase in 1 Hz EEG power (ANOVA, $F_{(4,184)} = 7.1$, $p < .00001$). For all other frequencies, patients generated smaller increases in power in the stimulation band across stimulation frequencies (ANOVA $F_{(1,184)} = 5.3$, $p = .02$). There was a statistically significant difference between patients and controls in response to alpha band (10 Hz) stimulation ($p = .036$, post-hoc unpaired t-test).

We also analyzed responses at harmonics of the stimulation frequencies (Fig. 5A). When we compared the responses during stimulation to eyes-closed baseline, we found robust increases in mean EEG power across channels for the stimulation frequency (first harmonic) at 20 and 40 Hz stimulation in both patients and controls. In healthy controls, we also found increases in mean EEG power for the second and third harmonics at 10 Hz stimulation and the second harmonic at 20 Hz stimulation (SnPM, $p < .05$). The responses at the harmonic frequencies were less pronounced in the patients and were only statistically significant in the second harmonic of the 10 Hz stimulation (SnPM, $p < .05$).

We examined the spatial topography of the SSVEP responses (Fig. 5B, leftmost panel). For the 10 Hz stimulation, controls had broad increases in 10 Hz power. There were also increases in 10 Hz power in patients, but these did not reach statistical significance. When we compared the increases in 10 Hz power from baseline to stimulation condition between patients and controls, we found a large cluster of central electrodes that showed greater increases in controls than in patients (SnPM suprathreshold cluster test, $p = .01$). At the 20 Hz harmonic response to 10 Hz stimulation, we saw significant increases in

power in anterior and posterior scalp in controls and posterior scalp only in patients (SnPM suprathreshold cluster test, $p \leq .0001$ and $p < .001$ respectively). At the 30 Hz harmonic response to 10 Hz stimulation, controls showed increases in a large cluster of central electrodes while patients showed a much smaller and spatially limited increase in power (SnPM suprathreshold cluster test, $p < .0001$ and $p = .037$).

In the 20 Hz stimulation condition, we found that controls showed a broad increase in 20 Hz power across the scalp (SnPM suprathreshold cluster test, $p < .0001$). In patients, the increase was most pronounced posteriorly and attenuated toward the front of the head (SnPM, suprathreshold cluster test $p = .01$). There was a cluster of central right channels that showed a greater 20 Hz power increases during 20 Hz stimulation in controls compared to patients (SnPM suprathreshold cluster test, $p = .028$). At the 40 Hz response, we saw a cluster of posterior central channels that increased in power in controls (SnPM suprathreshold cluster test, $p < .0001$) and a smaller such cluster in patients (SnPM suprathreshold cluster test, $p = .006$).

In the 40 Hz stimulation condition, we again found a central cluster of electrodes in controls that increased in power during photic stimulation (SnPM suprathreshold cluster test, $p < .0001$). For the patients, we saw two central electrodes with statistically significant increases (SnPM, $p = .046$). When comparing controls to patients directly, we saw a similar pattern to that observed in the in the 40 Hz harmonic of 10 Hz and 20 Hz stimulation with a central cluster of electrodes that was greater in controls but did not reach statistical significance.

We also tested if the response to stimulation varied in time in either controls or patients. For each stimulation frequency, we compared the first 12 s of stimulation ("early response") to the final 12 s of

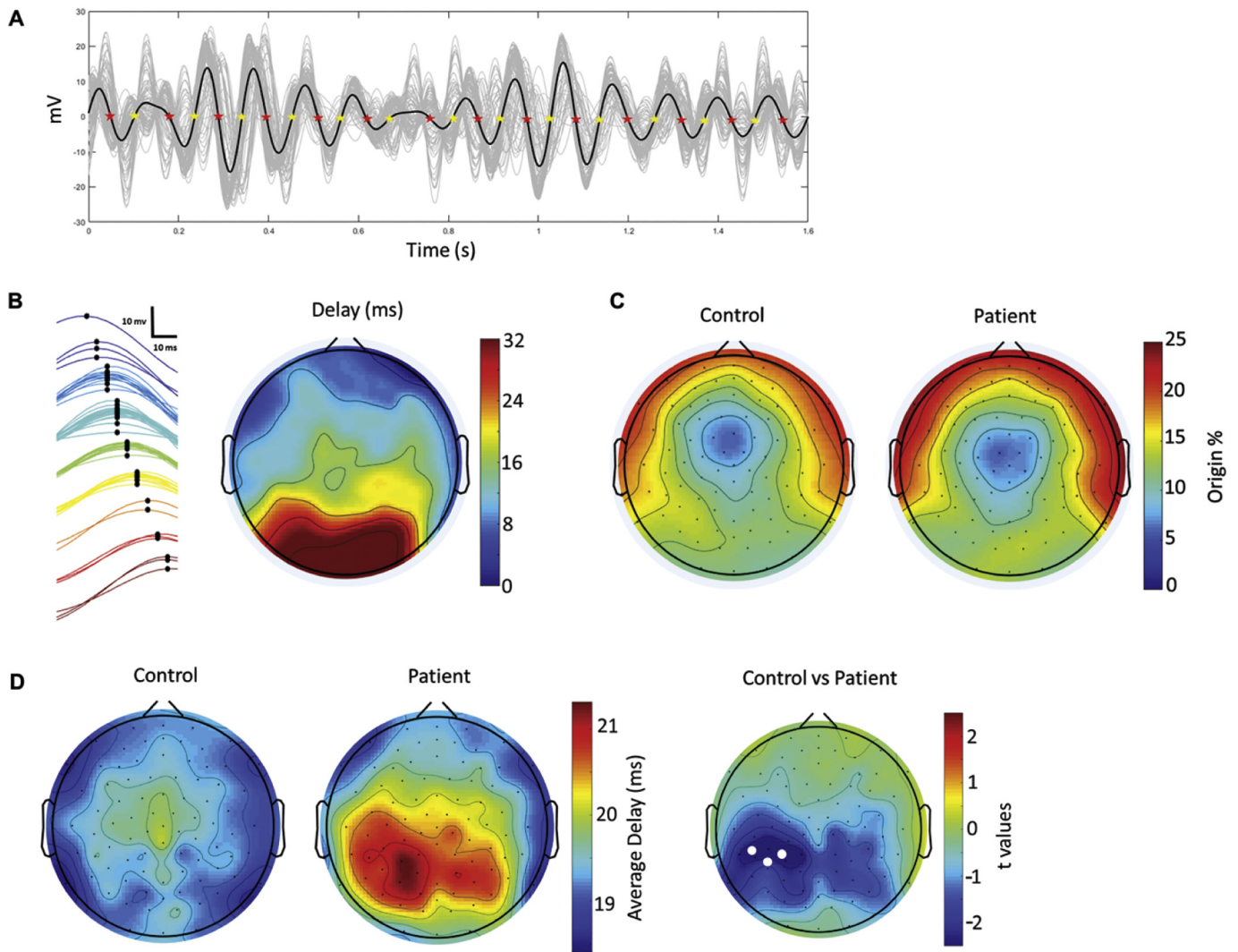


Fig. 3. Traveling alpha-wave analysis. A) A representative butterfly plot of 8–12 Hz filtered EEG data from a single subject. Each individual channel is plotted in gray. The average channel is plotted in black. The red stars indicate negative-going zero-crossings and the yellow stars indicate positive going zero-crossings. B) The left panel shows a representative positive alpha half-wave across channels. The channel tracings are colored based on their delay from the first identified peak. The black dots are the peaks. The right panel is a topographic map of the delays showing a clear anterior-to-posterior propagation of this wave. C) Alpha wave origin analysis. For each half wave, channels that peaked within the first ten percentile of the delays were considered to be the origin of that wave. The topoplots show the percentage of waves each channel originated. Both controls and patients showed more anterior and temporal origins with no statistically significant differences between the two groups. D) Alpha wave latency analysis. For each channel, we calculated the average delay across all waves. The left two panels are topoplots of this data for controls and patients. The right most topoplot is the t-values for each channel comparing between the groups. The white dots are a cluster of statistically significant channels where patients had higher delays than controls (statistical non-parametric mapping suprathreshold cluster test, $p = .045$).

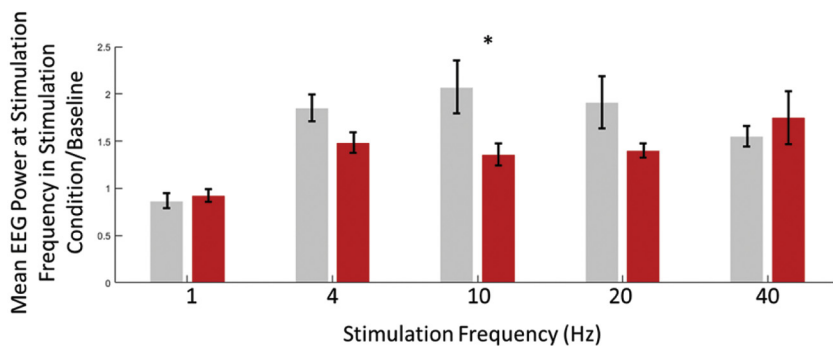


Fig. 4. Steady state visual evoked potentials. The bar graphs show average increase across all channels in the stimulation bands in controls (gray) and patients (red). Error bars are SEM. Patients showed significantly smaller increases in EEG power in the stimulation band in response during SSVEP ($F_{(1,184)} = 5.3$, $p = .02$). For both controls and FEP patients, stimulation at 1 Hz was statistically significantly less able to produce increases in the stimulation frequency band ($F_{(4,184)} = 7.1$, $p < .00001$). * post-hoc unpaired t-test, $p = .036$.

stimulation (“late response”) in each subject. We compared average power in the stimulation frequency band as well as in the 20, 30, and 40 Hz harmonics for 10 Hz stimulation and the 40 Hz harmonic for

20 Hz stimulation. We found no statistically significant differences between the early response and the late response within either group at any of the tested frequencies (paired t-tests, all p values $> .62$,

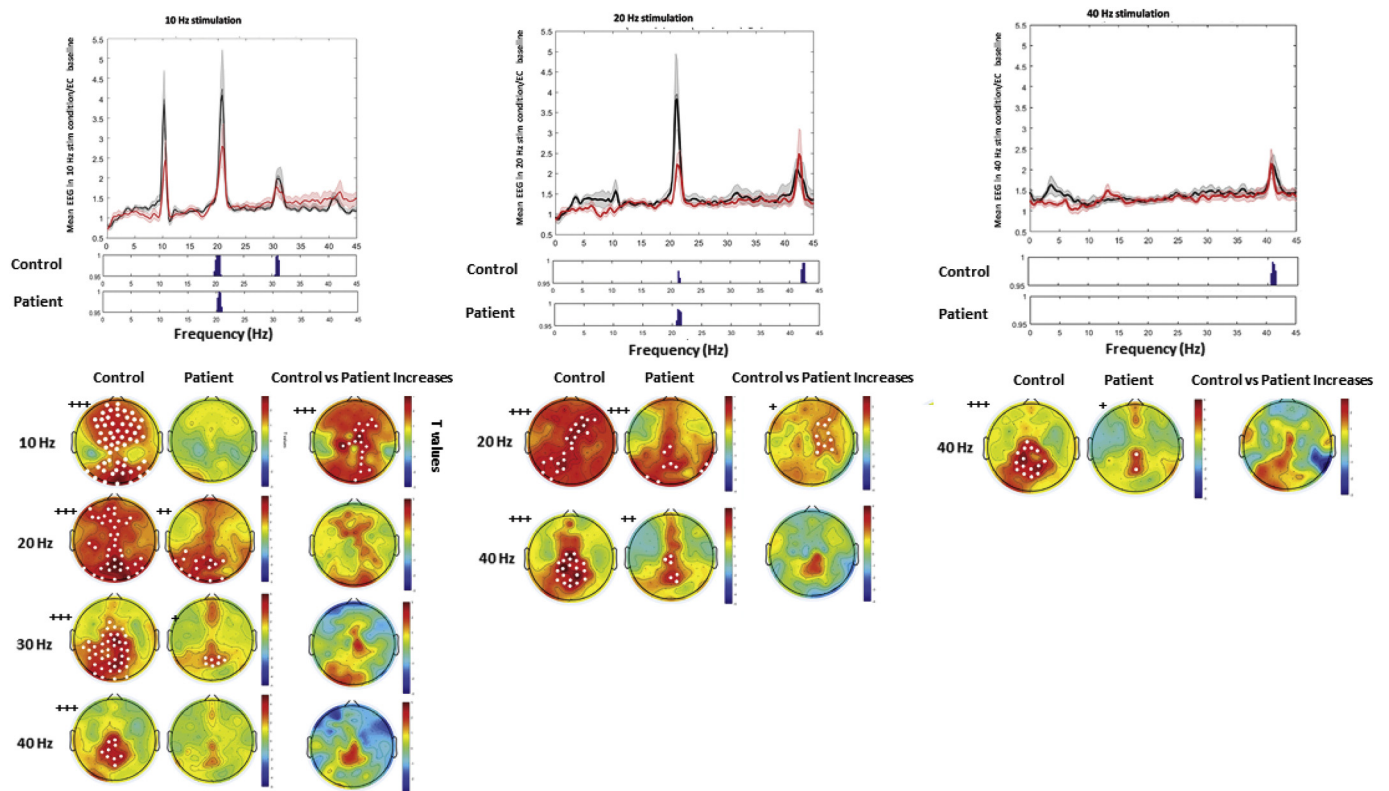


Fig. 5. Topographic and harmonic analysis of steady state visual evoked potentials. A) Mean power spectra across all channels from 0 to 49 Hz for each stimulation condition divided by eyes closed baseline for controls (black) and patients (red). Shaded areas are SEM at each point. Lower panels are statistically significant p-values by frequency bin between stimulation condition and baseline for controls and patients (SnPM). B) For the 10 Hz, 20 Hz, and 40 Hz stimulation there are topoplots of t-values for comparisons of, from left to right, “Control” - control stimulation vs Control baseline, “Patient” - patient stimulation vs patient baseline, “Control vs Patient Increases” - control stimulation/control baseline vs patient stimulation/patient baseline. White circles are statistically significant channels detected with SnPM suprathreshold cluster testing. + = $p < .05$, ++ = $p < .01$, +++ = $p < .001$. For each stimulation frequency, we show the comparison calculated in a 2 Hz bin centered on peak in Fig. 5a that is nearest to stimulation frequency (top row). For the 10 Hz stimulation, we repeated the analysis at the 20 Hz, 30 Hz, and 40 Hz harmonics. For the 20 Hz stimulation, we repeated the analysis at the 40 Hz harmonic.

corrected for multiple comparisons).

3.5. Ability to entrain to faster frequencies is relatively spared in patients with higher depression scores

We examined the relationship between aspects of resting alpha activity and SSVEP response and clinical characteristics such as symptom severity and duration of illness (Table 1). In this exploratory analysis, we found that the 40 Hz SSVEP response across all electrodes was positively correlated with the Depression Factor (Pearson's $r = 0.59$, $p = .02$, uncorrected). The ability to produce 40 Hz EEG power in response to visual stimulation at 10 Hz, 20 Hz, or 40 Hz was greater in patients with higher values for PANSS Depression factor (Fig. 6, $p = .023$, uncorrected). We note that this analysis was exploratory and does not survive multiple comparison correction ($p = .11$, Bonferroni adjusted), but may inform future hypothesis-driven work in this area. Individual peak alpha frequency and alpha wave speed during baseline were both correlated with 40 Hz stimulation response ($r = 0.52$, $p = .046$ and $r = 0.61$, $p = .009$ respectively). In contrast with the findings for the PANSS Depression factor, the 40 Hz SSVEP response across all electrodes was negatively correlated with use of antidepressant medication (Pearson's $r = -0.55$, $p = .033$, uncorrected).

4. Discussion

In this study, we conducted a high-density EEG analysis of resting alpha frequency and alpha, beta and gamma SSVEP response in a transdiagnostic sample of FEP patients. This approach allowed us to

probe subtle topographic abnormalities in cortical and thalamic function in a highly symptomatic population. We report slowing of the peak alpha rhythm in FEP patients that was most notable over central, temporal and occipital cortex. Contrary to our hypotheses, we did not find decreases in alpha power, even in analyses restricted to channels used in previous reports (Goldstein et al., 2015). This may be related to the fact that decreased alpha power has previously been shown to be associated with negative symptoms in schizophrenia (Merrin and Floyd, 1996; Sponheim et al., 2000). Our study population had lower amounts of negative symptoms than these previous reports (PANSS negative subscale score of 16.0 ± 0.9 , compared to 20.2 in Goldstein et al. for example)(Goldstein et al., 2015). We also found that, in line with previous work, alpha waves generated during quiet rest originate in frontal regions (Ito et al., 2005; Halgren et al., 2017). Origination of alpha waves appears to be unaffected by psychotic illness while propagation of alpha waves across the scalp is impaired. Finally, we show that patients are less able to entrain to alpha, beta, and gamma responses suggesting an abnormality at or distal to the level of the thalamus that is not specific to alpha frequencies.

4.1. Alpha rhythm and SSVEP abnormalities in first-episode psychosis suggest both cortical and thalamic dysfunction

Resting state EEG alpha activity likely arises from coordinated activity of frontal alpha generators, thalamic structures including the LGN and pulvinar nuclei, and downstream posterior cortex (Hughes and Crunelli, 2005; Halgren et al., 2017; Vijayan and Kopell, 2012). Therefore, our data provides several lines of evidence that the alpha

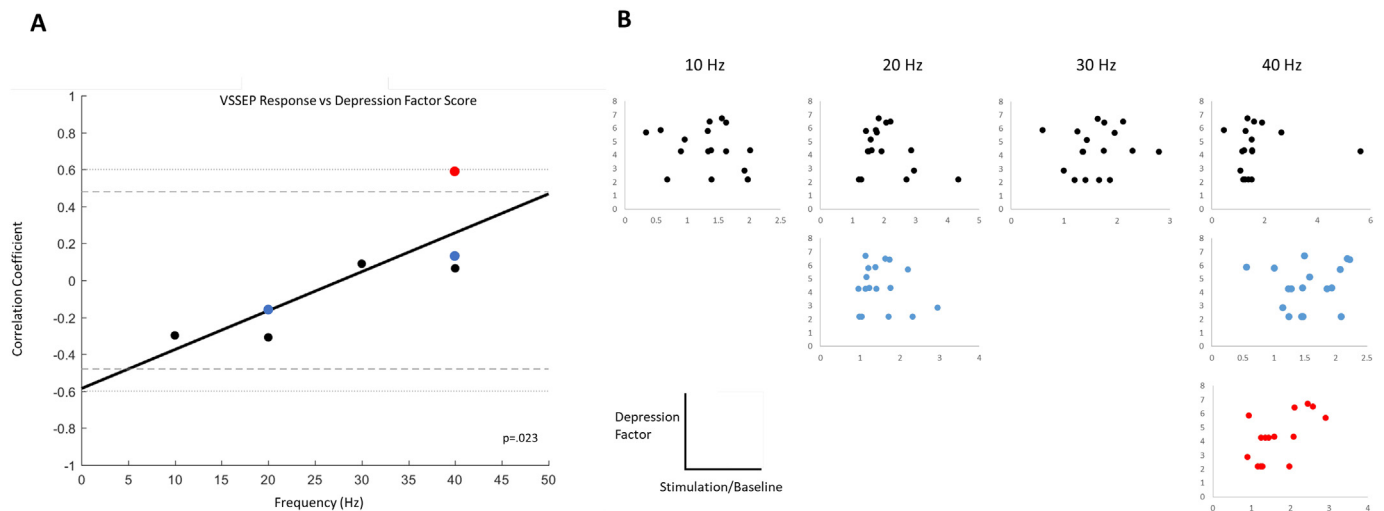


Fig. 6. A) Scatter plot of correlation coefficients between EEG power at 10, 20, 30, and 40 Hz in 10 Hz stimulation (black), 20 Hz stimulation (blue), and 40 Hz stimulation (red) and the PANSS depression score. The dashed line is $p = .05$ for the individual correlations and the dotted line is $p = .01$. The trendline has an R value of 0.82 and p value of 0.023 (uncorrected). Of note, individual peak alpha frequency and alpha wave speed during baseline were both correlated with 40 Hz stimulation response (red dot, $R = 0.52$, $p = .046$ and $R = 0.61$, $p = .009$ respectively). B) The individual scatter plots that were used to generate the correlation coefficients in A. The y-axes are the Depression Factor scores and the x-axes are the stimulation condition divided by the baseline condition at the specified frequency band. As in A, the color of the dots is used to distinguish the stimulation frequency.

findings in psychotic disorders may be related to aberrant corticocortical connectivity, thalamic dysfunction and aberrant thalamocortical connectivity. We did not find significantly decreased peak alpha frequency in frontal and temporal regions where most alpha waves originated. This suggests that frontal cortical alpha pacemakers are relatively normal in these patients. Delayed propagation from these anterior generators to central regions suggests that short-range supragranular corticocortical connections are impaired (Halgren et al., 2017). In addition, we found that alpha slowing was most notable posteriorly, downstream from both short-range corticocortical connections and long range input from thalamic nuclei.

It is unclear to what extent steady-state responses in the alpha band are caused by entrainment of the endogenous alpha rhythm (Keitel et al., 2014; Labecki et al., 2016; Notbohm et al., 2016). It is likely that large scale cortical oscillations are driven by the LGN and by connectivity from occipital cortex toward anterior regions rather than relying on a frontal pacemaker as in endogenous alpha activity (Hoftman et al., 2015; Krolak-Salmon et al., 2003; Burkitt et al., 2000). In this paper, we report smaller areas of entrainment at multiple frequencies and in particular decreases over central areas of the scalp. Anatomical studies indicate that the LGN is structurally intact in schizophrenia, although it may be abnormal in patients with affective disorders (Dorph-Petersen et al., 2009; Selemon and Begović, 2007). This suggests that the observed SSVEP deficits are related to previously reported decreases in neuron number in visual cortex in schizophrenia or to previously reported aberrant connectivity between LGN and downstream occipital cortex (Anticevic et al., 2014; Dorph-Petersen et al., 2007). The decrease in 10 Hz SSVEP power with persevered alpha power may be explained by the relative importance of the occipital cortex in generating and sustaining the SSVEP response compared to the endogenous alpha rhythm.

Many different stimuli have been used to elicit the SSVEP response (Vialatte et al., 2010). The choice of stimuli is thought to influence the relative recruitment of magnocellular and parvocellular pathways (Vialatte et al., 2010). Within our photic stimulation paradigm higher frequency of stimulation has been reported to favor activation of the magnocellular pathway although this is controversial (Vialatte et al., 2010; Brenner et al., 2009). Our SSVEP results are broadly consistent with past work which has shown decreased SSVEP response in schizophrenia at or above 10 Hz stimulation with preserved response at

frequencies below 10 Hz (Goldstein et al., 2015; Rice et al., 1989; Jin et al., 1990; Krishnan et al., 2005; Brenner et al., 2009; Clementz et al., 2004; Jin et al., 2000).

Given the uncertainty about the generation and maintenance of both endogenous alpha rhythm and SSVEP responses, caution should be taken when applying our results to experimental models of schizophrenia. Amphetamine, which acts to increase dopaminergic tone, has been used as a model of psychosis (Fink, 1968). However, amphetamine administration does not appear to produce reliable changes in alpha activity (Fink, 1968). Data from slice studies and computer modeling studies have highlighted the role of metabotropic glutamate receptors and muscarinic acetylcholine receptors in shaping thalamic alpha activity (Hughes and Crunelli, 2005; Vijayan and Kopell, 2012; Hughes et al., 2004). In particular, thalamic alpha rhythm may be slowed by decreased cholinergic tone (Hughes and Crunelli, 2005). Hypofunction of *N*-methyl-D-aspartate receptor (NMDAR) on GABA-ergic interneurons has been implicated in the pathogenesis of schizophrenia (Nakazawa et al., 2012). Consistent with this model and with our own results, ketamine, a NMDAR antagonist, has been shown to decrease alpha activity and also to exacerbate psychotic symptoms (Lahti et al., 1995; Blain-Moraes et al., 2014). Furthermore, sub-anesthetic doses of ketamine disrupt alpha-band anterior-to-posterior connectivity which is line with our findings of delayed alpha wave traveling (Nakazawa et al., 2012). Taken together, this suggests that our findings are broadly consistent with glutamatergic and GABA-ergic models of schizophrenia. The GABA-ergic interneurons implicated in the above models are largely parvalbumin positive (Nakazawa et al., 2012). Methylazoy-methanol acetate (MAM) has been used to produce a developmental model of schizophrenia in rats (Lodge et al., 2009). MAM-exposed rats have several neurologic abnormalities including a notable loss of parvalbumin-positive interneurons (Lodge et al., 2009). Previous work has not shown clear differences in spontaneous neural oscillations in MAM rats compared to control animals (Lodge et al., 2009). However, evoked oscillatory activity is reduced in these animals and therefore future studies should determine if SSVEP are disrupted (Lodge et al., 2009).

4.2. Preserved SSVEP response to gamma frequency may be a state marker of depression in patients with psychotic illness

Previous studies have reported mixed results when examining the

relationship between resting-state alpha parameters and clinical features in schizophrenia. One paper suggested that peak alpha frequency may be a marker of disease chronicity (Goldstein et al., 2015). However, this was a cross-sectional analysis. There are fewer data about SSVEP and symptom burden, with one study suggesting a possible relationship between hallucinations and SSVEP power that did not achieve statistical significance (Krishnan et al., 2005). Another study found that clozapine increased SSVEP responses in responders (Jin et al., 1995). We did find evidence that entrainment of gamma rhythm in response to steady-state visual stimulation is stronger in patients with depressive symptoms. While our study was not designed to distinguish first-episode affective psychosis from first-episode non-affective psychosis and we emphasize that diagnosis often changes during and after a first episode of psychosis we nonetheless note that our finding is in agreement with a small, but growing, body of evidence that beta and/or gamma SSVEP responses may be different in patients with schizophrenia compared to patients with other psychotic illnesses (Parker et al., 2018). However, we note that our finding was specific for the Depression symptom factor and not for diagnosis. Nor did we find a similar association with the Excited symptom factor which would presumably be elevated in manic patients with bipolar disorder. Rather, since all of our patients had a psychotic disorder, the presence of depression may identify a state that allows the thalamus and occipital cortex to entrain to gamma stimulation perhaps mitigating or compensating for thalamocortical dysconnectivity.

4.3. Traveling waves as a tool to probe brain dysfunction

Neural oscillations vary across space and time. By including analyses of wave-traveling we can begin to distinguish between dysfunctions within oscillatory pacemakers and others in corticocortical connections which act in concert to synchronize neural activity over the cortex (Nunez and Srinivasan, 2006a). Such analyses may be particularly relevant for understanding psychotic disorders which are associated with multiple subtle anatomical and genetic abnormalities. Our findings suggest that traveling wave analyses may be used in concert with standard EEG analyses to parse out distinct neural pathologies associated with specific symptoms and perhaps responsive to different treatments.

5. Limitations

This study has limitations that should be considered when interpreting our findings. We did not track eye movements and it is possible that there were differences in fixation between the two groups. Our study was not designed to measure the effect of medication on oscillations nor was it designed to identify diagnostic biomarkers. Our findings may be related to or mediated by medications however we note that we found no correlations between medications and EEG findings in our study and previous work have not consistently reported medication-mediated effects in alpha rhythm or SSVEP response (Goldstein et al., 2015; Butler and Javitt, 2005). Furthermore, previous work a study of psychiatric patients without psychotic disorders who used antipsychotic medication (for example, as an adjunctive treatment for depression) had alpha activity that was indistinguishable from healthy controls (Goldstein et al., 2015). It may be that patients with schizophrenia and patients with bipolar disorder have distinct neuropathologies that give rise to overlapping but distinct abnormal alpha rhythm and SSVEP responses. In addition, EEG has poor spatial resolution which makes precise localization of abnormal oscillatory activity difficult. Furthermore, EEG cannot directly measure thalamic activity (Nunez and Srinivasan, 2006b). As in previous work using EEG to model the cortical correlates of large-scale oscillatory activity, our findings about alpha wave origination and propagation should be interpreted in light of the limitations and theoretical assumptions inherent in EEG source modeling (Murphy et al., 2009). This study is cross-sectional which limits

our ability to draw inferences about relationships between abnormal EEG oscillations and clinical symptoms. Future studies should use a longitudinal repeated measures approach to investigate SSVEP in patients with psychotic illness. In particular, investigating patients with bipolar depression and depression with psychotic features, whose clinical states vary over time will allow us to further elucidate both state and trait connections between mood symptoms and gamma SSVEP entrainment.

Disclosures

Dr. Murphy and Dr. Öngür report no biomedical financial interests or potential conflicts of interest.

Acknowledgments

This work was funded by the Stanley Center at the Broad Institute of Harvard and MIT Psychiatric Genetics and Neuroscience fellowship and the Harvard Medical School Department of Psychiatry Livingston Award (Michael Murphy). This data was previously presented in an abbreviated form on a poster at the Society of Biological Psychiatry 2018 meeting. The authors wish to thank Robert Stickgold and Diego Pizzagalli for their helpful comments on this manuscript.

References

- Anticevic, A., et al., 2014. Mediodorsal and visual thalamic connectivity differ in schizophrenia and bipolar disorder with and without psychosis history. *Schizophr. Bull.* 40, 1227–1243.
- Bahramsharif, A., et al., 2013. Propagating neocortical gamma bursts are coordinated by traveling alpha waves. *J. Neurosci.* 33, 18849–18854.
- Basar, E., et al., 2012. Brain's alpha activity is highly reduced in euthymic bipolar disorder patients. *Cogn. Neurodyn.* 6, 11–20.
- Becker, R., Van De Ville, D., Kleinschmidt, A., 2017. Alpha oscillations reduce temporal long-range dependence in spontaneous human brain activity. *J. Neurosci.* <https://doi.org/10.1523/JNEUROSCI.0831-17.2017>. 0831–17.
- Blain-Moraes, S., Lee, U., Ku, S., Noh, G., Mashour, G.A., 2014. Electroencephalographic effects of ketamine on power, cross-frequency coupling, and connectivity in the alpha bandwidth. *Front. Syst. Neurosci.* 8 (1–9).
- Boutros, N.N., et al., 2008. The status of spectral EEG abnormality as a diagnostic test for schizophrenia. *Schizophr. Res.* 99, 225–237.
- Brenner, C.A., et al., 2009. Steady state responses: electrophysiological assessment of sensory function in schizophrenia. *Schizophr. Bull.* 35, 1065–1077.
- Burkitt, G.R., Silberstein, R.B., Cadusch, P.J., Wood, A.W., 2000. Steady-state visual evoked potentials and travelling waves. *Clin. Neurophysiol.* 111, 246–258.
- Butler, P.D., Javitt, D.C., 2005. Early-stage visual processing deficits in schizophrenia. *Curr. Opin. Psychiatry* 18, 151–157.
- Clementz, B., Sponheim, S., Iacono, W., Beiser, M., 1994. Resting EEG in first-episode schizophrenia patients, bipolar psychosis patients, and their first-degree relatives. *Psychophysiology* 31, 486–494.
- Clementz, B.A., Keil, A., Kissler, J., 2004. Aberrant brain dynamics in schizophrenia: delayed buildup and prolonged decay of the visual steady-state response. *Cogn. Brain Res.* 18, 121–129.
- Corvin, A., Harold, D., 2015. Biomarkers for psychosis: the molecular genetics of psychosis. *Curr. Behav. Neurosci. Rep.* 2, 112–118.
- Craddock, N., Owen, M.J., 2007. Rethinking psychosis: the disadvantages of a dichotomous classification now outweigh the advantages. *World Psychiatry* 6, 84–91.
- Dorph-Petersen, K.-A., Pierri, J.N., Wu, Q., Sampson, A.R., Lewis, D.A., 2007. Primary visual cortex volume and Total neuron number are reduced in schizophrenia. *J. Comp. Neurol.* 501, 290–301.
- Dorph-Petersen, K.-A., et al., 2009. Volume and neuron number of the lateral geniculate nucleus in schizophrenia and mood disorders. *Acta Neuropathol.* 117, 369–384.
- Fink, M., 1968. EEG and Human Psychopharmacology. *Annu. Rev. Pharmacol.* 241–258.
- Goldstein, M.R., Peterson, M.J., Sanguinetti, J.L., Tononi, G., Ferrarelli, F., 2015. Topographic deficits in alpha-range resting EEG activity and steady state visual evoked responses in schizophrenia. *Schizophr. Res.* 168, 145–152.
- Halgren, M., et al., 2017. The Generation and Propagation of the Human Alpha Rhythm ([bioRxiv 202564](https://doi.org/10.1101/202564)). <https://doi.org/10.1101/202564>.
- Hanslmayr, S., Gross, J., Klimesch, W., Shapiro, K.L., 2011. The role of alpha oscillations in temporal attention. *Brain Res. Rev.* 67, 331–343.
- Harris, A., Melkonian, D., Williams, L., Gordon, E., 2006. Dynamic spectral analysis findings in first episode and chronic schizophrenia. *Int. J. Neurosci.* 116, 223–246.
- Hirano, Y., et al., 2015. Spontaneous gamma activity in schizophrenia. *JAMA Psychiatry* 72, 813–821.
- Hoftman, G.D., et al., 2015. Altered cortical expression of GABA-related genes in schizophrenia: illness progression vs developmental disturbance. *Schizophr. Bull.* 41, 180–191.
- Hughes, S.W., Crunelli, V., 2005. Thalamic mechanisms of EEG alpha rhythms and their

- pathological implications. *Neuroscientist* 11, 357–372.
- Hughes, S.W., et al., 2004. Synchronized oscillations at α and θ frequencies in the lateral geniculate nucleus. *Neuron* 42, 253–268.
- Ito, J., Nikolaev, A.R., Van Leeuwen, C., 2005. Spatial and temporal structure of phase synchronization of spontaneous alpha EEG activity. *Biol. Cybern.* 92, 54–60.
- Jin, Y., et al., 1990. Abnormal EEG responses to photic stimulation in schizophrenic patients. *Schizophr. Bull.* 16, 627–634.
- Jin, Y., Potkin, S.G., Sandman, C., 1995. Clozapine increases EEG photic driving in clinical responders. *Schizophr. Bull.* 21, 263–268.
- Jin, Y., Potkin, S.G., Sandman, C.A., Bunney, W.E., 1997. Electroencephalographic photic driving in patients with schizophrenia and depression. *Biol. Psychiatry* 41, 496–499.
- Jin, Y., Castellanos, A., Solis, E.R., Potkin, S.G., 2000. EEG resonant responses in schizophrenia: a photic driving study with improved harmonic resolution. *Schizophr. Res.* 44, 213–220.
- Karadağ, F., et al., 2003. Quantitative EEG analysis in obsessive compulsive disorder. *Int. J. Neurosci.* 113, 833–847.
- Karson, C.N., Coppola, R., Daniel, D.G., Weinberger, D.R., 1988. Computerized EEG in schizophrenia. *Schizophr. Bull.* 14, 193–197.
- Kay, S.R., Fiszbein, A., Opler, L.A., 1987. The Positive and Negative Syndrome Scale (PANSS) for schizophrenia. *Schizophr. Bull.* 13, 261–276.
- Keitel, C., Quigley, C., Ruhnau, P., 2014. Stimulus-driven brain oscillations in the alpha range: entrainment of intrinsic rhythms or frequency-following response? *J. Neurosci.* 34, 10137–10140.
- Krishnan, G.P., et al., 2005. Steady state visual evoked potential abnormalities in schizophrenia. *Clin. Neurophysiol.* 116, 614–624.
- Krolak-Salmon, P., et al., 2003. Human lateral geniculate nucleus and visual cortex respond to screen flicker. *Ann. Neurol.* 53, 73–80.
- Labecki, M., et al., 2016. Nonlinear origin of SSVEP spectra—a combined experimental and modeling study. *Front. Comput. Neurosci.* 10, 1–10.
- Lahti, A., Koffel, B., LaPorte, D., Tamminga, C., 1995. Subanesthetic doses of ketamine stimulate psychosis in schizophrenia. *Neuropsychopharmacology* 13, 9–19.
- Lisman, J.E., et al., 2008. Circuit-based framework for understanding neurotransmitter and risk gene interactions in schizophrenia. *Trends Neurosci.* 31, 234–242.
- Llinas, R.R., Ribary, U., Jeanmonod, D., Kronberg, E., Mitra, P.P., 1999. Thalamocortical dysrhythmia: a neurological and neuropsychiatric syndrome characterized by magnetoencephalography. *Proc. Natl. Acad. Sci.* 96, 15222–15227.
- Lodge, D.J., Behrens, M.M., Grace, A.A., 2009. A loss of Parvalbumin-containing interneurons is associated with diminished oscillatory activity in an animal model of schizophrenia. *J. Neurosci.* 29, 2344–2354.
- Manjarrez, E., Vázquez, M., Flores, A., 2007. Computing the center of mass for traveling alpha waves in the human brain. *Brain Res.* 1145, 239–247.
- Massimini, M., 2004. The sleep slow oscillation as a traveling wave. *J. Neurosci.* 24, 6862–6870.
- Merrin, E.L., Floyd, T.C., 1996. Negative symptoms and EEG alpha in schizophrenia: a replication. *Schizophr. Res.* 19, 151–161.
- Millett, D., 2001. Hans Berger: from psychic energy to the EEG. *Perspect. Biol. Med.* 44, 522–542.
- Müller, M.M., Hübner, R., 2002. Can the spotlight of attention be shaped like a donut? Evidence from steady-state visual evoked potentials. *Psychol. Sci.* 13, 119–124.
- Murphy, M., et al., 2009. Source modeling sleep slow waves. *Proc. Natl. Acad. Sci.* 106, 1608–1613.
- Nakazawa, K., et al., 2012. GABAergic interneuron origin of schizophrenia pathophysiology. *Neuropharmacology* 62, 1574–1583.
- Narayanan, B., et al., 2014. Resting state electroencephalogram oscillatory abnormalities in schizophrenia and psychotic bipolar patients and their relatives from the bipolar and schizophrenia network on intermediate phenotypes study. *Biol. Psychiatry* 76, 456–465.
- Nichols, T.E., Holmes, A.P., 2001. Nonparametric permutation tests for {PET} functional neuroimaging experiments: a primer with examples. *Hum. Brain Mapp.* 15, 1–25.
- Notbohm, A., Kurths, J., Herrmann, C.S., 2016. Modification of brain oscillations via rhythmic light stimulation provides evidence for entrainment but not for superposition of event-related responses. *Front. Hum. Neurosci.* 10.
- Nunez, P.L., Srinivasan, R., 2006a. A theoretical basis for standing and traveling brain waves measured with human EEG with implications for an integrated consciousness. *Clin. Neurophysiol.* 117, 2424–2435.
- Nunez, P.L., Srinivasan, R., 2006b. *Electric Fields of the Brain*. Oxford University Press <https://doi.org/10.1093/acprof:oso/9780195050387.001.0001>.
- Parker, D., et al., 2018. 148. Auditory and visual EEG validators of psychosis biotypes, findings from bipolar-schizophrenia network on intermediate phenotypes (B-SNIP) consortium. *Biol. Psychiatry* 83, S60–S61.
- Pascual-Marqui, R.D., 2002. Standardized low-resolution brain electromagnetic tomography (sLORETA): technical details. *Methods Find. Exp. Clin. Pharmacol.* 24 (Suppl D), 5–12.
- Prinz, P.N., Vitiello, M.V., 1989. Dominant occipital (alpha) rhythm frequency in early stage Alzheimer's disease and depression. *Electroencephalogr. Clin. Neurophysiol.* 73, 427–432.
- Rice, D.M., et al., 1989. EEG alpha photic driving abnormalities in chronic schizophrenia. *Psychiatry Res.* 30, 313–324.
- Ripke, S., et al., 2014. Biological insights from 108 schizophrenia-associated genetic loci. *Nature* 511, 421–427.
- Samaha, J., Bauer, P., Cimaroli, S., Postle, B.R., 2015. Top-down control of the phase of alpha-band oscillations as a mechanism for temporal prediction. *Proc. Natl. Acad. Sci.* 112, 8439–8444.
- Schreckenberger, M., et al., 2004. The thalamus as the generator and modulator of EEG alpha rhythm: a combined PET/EEG study with lorazepam challenge in humans. *Neuroimage* 22, 637–644.
- Selemon, L.D., Begović, A., 2007. Stereologic analysis of the lateral geniculate nucleus of the thalamus in normal and schizophrenic subjects. *Psychiatry Res.* 151, 1–10.
- Shinn, A.K., et al., 2017. McLean OnTrack: a transdiagnostic program for early intervention in first-episode psychosis. *Early Interv. Psychiatry* 11, 83–90.
- Sponheim, S.R., Clementz, B.A., Iacono, W.G., Beiser, M., 2000. Clinical and biological concomitants of resting state EEG power abnormalities in schizophrenia. *Biol. Psychiatry* 48, 1088–1097.
- Tadel, F., Baillet, S., Mosher, J.C., Pantazis, D., Leahy, R.M., 2011. Brainstorm: a user-friendly application for MEG/EEG analysis. *Comput. Intell. Neurosci.* 2011.
- Tohen, M., et al., 2003. The McLean-Harvard first-episode mania study: prediction of recovery and first recurrence. *Am. J. Psychiatry* 160, 2099–2107.
- van der Gaag, M., et al., 2006. The five-factor model of the positive and negative syndrome scale II: a ten-fold cross-validation of a revised model. *Schizophr. Res.* 85, 280–287.
- Vialatte, F.B., Maurice, M., Dauwels, J., Cichocki, A., 2010. Steady-state visually evoked potentials: focus on essential paradigms and future perspectives. *Prog. Neurobiol.* 90, 418–438.
- Vijayan, S., Kopell, N.J., 2012. Thalamic model of awake alpha oscillations and implications for stimulus processing. *Proc. Natl. Acad. Sci.* 109, 18553–18558.
- Wada, Y., Takizawa, Y., Yamaguchi, N., 1995. Abnormal photic driving responses in never-medicated schizophrenia patients. *Schizophr. Bull.* 21, 111–115.
- Wallwork, R.S., Fortgang, R., Hashimoto, R., Weinberger, D.R., Dickinson, D., 2012. Searching for a consensus five-factor model of the positive and negative syndrome scale for schizophrenia. *Schizophr. Res.* 137, 246–250.
- Yoshimura, M., et al., 2007. A pharmacology-EEG study on antipsychotic drugs in healthy volunteers. *Psychopharmacology* 191, 995–1004.